Acta Cryst. (1953). **6**, 273

X-ray Analysis of the Ferroelectric Transition in KH_2PO_4*

BENJAMIN CHALMERS FRAZER AND RAY PEPINSKY

Department of Physics, The Pennsylvania State College, State College, Pa., U.S.A.

(*Received* 29 *August* 1952)

The crystal structure of KH_2PO_4 was examined by X-ray analysis just above and just below the ferroelectric transition at 122° K. Observation temperatures were 126° K. for the tetragonal $I\bar{4}2d$ (or $F\bar{4}d2$) structure and 116° K. for the orthorhombic Fdd structure. Complete sets of intensities were measured from oscillation photographs for (HHL) reflections in $F\bar{4}d2$ and ($HK0$) and (HHL) reflections in Fdd. In the case of ($HK0$) observations, an electric field was applied parallel to the ferroelectric c axis to eliminate splitting and non-equivalent superposition. The field was not required in the (HHL) case. The structures were solved by Fourier projections and refined by difference syntheses and least-squares analyses. Values of the reliability index R were 12·1 for (HHL) in $F\bar{4}d2$, 13·5 for ($HK0$) in Fdd, and 11·8 for (HHL) in Fdd.

The hydrogen bonds were found to contract from a room-temperature distance of 2·53 Å to 2·44 Å at 126° K., and to expand in the transition to 2·51 Å at 116° K. A K displacement of 0·08 Å relative to the nearest P's, or 0·05 Å relative to the corresponding O_4 tetrahedra, was observed parallel to the c axis. The O_4 tetrahedra were found to be more regular than at room temperature; below the transition temperature the central P's were displaced by 0·03 Å within the tetrahedra. Thermal vibrations were anisotropic, with maximum displacement along the c axis. The much discussed ordering of the hydrogens appears to be in accord with the observed structural changes.

1. Introduction

Almost all of the numerous studies of potassium dihydrogen phosphate which have appeared in the literature in recent years have been concerned either with the piezoelectric properties of this crystal at room temperature or the transition to a ferroelectric state at 122° K. The ferroelectric transition was discovered by Busch & Scherrer (1935), and subsequently these investigators and their associates at Zürich contributed much of what is now known about the dielectric behavior of this crystal and its several isomorphs. Despite the considerable attention the dihydrogen phosphate ferroelectrics have received, no entirely satisfactory explanation has been advanced for their behavior. The most generally accepted theory is that of Slater (1941). While this theory may be correct in some of its main features, it falls short of a full explanation.

Accurate information on the crystal structure of a ferroelectric is fundamental to the achievement of understanding its ferroelectric properties. An accurate determination of the crystal structure of KH_2PO_4 at room temperature was made more than twenty years ago by West (1930), and it was on this work that the Slater theory was based. At the time Slater published his theory no X-ray study had been carried through on the structure below the ferroelectric transition (Curie) temperature. Subsequent X-ray studies by de Quervain (1944) and by Ubbelohde & Woodward (1947) established a change at the Curie point from the room-temperature tetragonal $I\bar{4}2d$ symmetry to that of the orthorhombic space group Fdd. These investigators also measured the alterations in the lattice, and reported changes in X-ray intensities for several of the diffraction maxima. The latter were not correlated with a redistribution of electron density, however, although de Quervain did propose a model for the orthorhombic structure, some features of which have been found to be correct.

The purpose of the present investigation was to determine by X-ray analysis the structure of KH_2PO_4 at temperatures just above and just below the Curie point. Some measurable changes in interatomic distances were to be expected between the structure as determined by West at room temperature and that just above the transition point, and these could be expected to provide insight into the nature of the transition. The structure just above the transition point affords information on temperature corrections for the atomic scattering curves in this temperature range, and is preferable to the room-temperature structure for deductions of the mechanism of the transition.

The X-ray observations on which the results discussed here are based were recorded photographically at the temperature 116° K. and 126° K. using a low-temperature goniometer designed and constructed in this laboratory (Frazer & Pepinsky, 1950).

* Research conducted under Contract No. 36-039, SC-21, with Signal Corps Engineering Laboratories, and under a fellowship grant from the Gulf Research and Development Co., Pittsburgh, Pa. Neutron diffraction study conducted at Brookhaven National Laboratory. Computations on X-RAC supported by Contract No. N6onr-26916 with the Office of Naval Research.

2. The room-temperature structure

(*A*) *Summary of West's structure*

Potassium dihydrogen phosphate crystallizes in the tetragonal space group $I\bar{4}2d$ with 4 'molecules' of KH_2PO_4 per unit cell. The cell dimensions found by West (1930), and somewhat more accurate values observed later by Ubbelohde & Woodward (1947), are as follows:

$a = b$ (Å)	c (Å)	
7·43	6·97	(West)
7·434	6·945	(Ubbelohde & Woodward)

The atomic coordinates* in this unit cell are given in Table 1.

Table 1. *Coordinates in* $I\bar{4}2d$

4 P: $0, 0, 0;\ \frac{1}{2}, 0, \frac{1}{4};\ \frac{1}{2}, \frac{1}{2}, \frac{1}{2};\ 0, \frac{1}{2}, \frac{3}{4}$.

4 K: $0, 0, \frac{1}{4};\ \frac{1}{2}, 0, \frac{3}{4};\ \frac{1}{2}, \frac{1}{2}, 0;\ 0, \frac{1}{2}, \frac{1}{4}$.

16 O: $x, y, z;\ \frac{1}{2}-x, y, \frac{1}{4}-z;$
$\bar{x}, \bar{y}, z;\ \frac{1}{2}+x, \bar{y}, \frac{1}{4}-z;$
$\bar{y}, x, \bar{z};\ \frac{1}{2}+y, x, \frac{1}{4}+z;$
$y, \bar{x}, \bar{z};\ \frac{1}{2}-y, \bar{x}, \frac{1}{4}+z;$
+8 similar points about $\frac{1}{2}, \frac{1}{2}, \frac{1}{2}$.

8 H: $\frac{1}{4}, u, \frac{1}{8};\ u, \frac{3}{4}, \frac{7}{8};\ \frac{3}{4}, \bar{u}, \frac{1}{8};\ \bar{u}, \frac{1}{4}, \frac{7}{8};$
+ similar points about $\frac{1}{2}, \frac{1}{2}, \frac{1}{2}$.

West found the oxygen parameters to be

$$x = 0{\cdot}0805,\ y = 0{\cdot}144,\ z = 0{\cdot}139\ .$$

These values resulted in a fairly regular PO_4 tetrahedron with P, O = 1·56 Å, O, O = 2·46 Å, and O, O′ = 2·60 Å, where the O, O distance is between oxygens of the same elevation in the c direction and O, O′ is that between those of opposite elevation (relative to the central P atom). Each K was found to be surrounded by eight practically equidistant oxygen neighbors:

K, O = 2·79 Å for the four O's of PO_4 groups

above and below K, and

K, O′ = 2·81 Å for the four other neighbors.

The distance between nearest oxygens of adjacent PO_4 groups was found to be 2·54 Å which strongly suggested the existence of hydrogen bonds. Because of this distance and the improbability of the alternative 8-fold position in $I\bar{4}2d$, West chose the 8-fold position for hydrogen as shown in Table 1. The logical assumption, that the hydrogen would be located on the line of centers of the oxygens, then led to his assignment of $u = 0{\cdot}144$ as being probable for the hydrogen parameter.

A schematic projection of the structure on (001) is shown in Fig. 1. The large circles represent potassium atoms and the small circles the oxygens. The phosphorus positions are omitted since their positions at

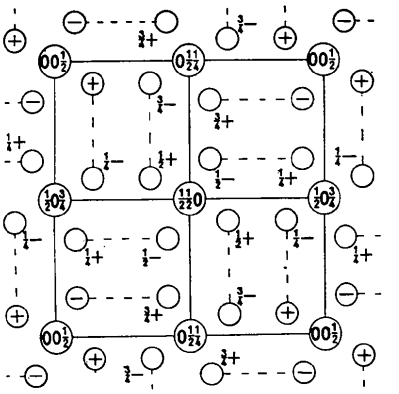

Fig. 1. Schematic projection of tetragonal KH_2PO_4 on (001). Large circles: potassium; small circles: oxygen.

distances $\frac{1}{2}c$ above and below the potassiums are obvious. The broken lines indicate the hydrogen bonds presumed to connect the PO_4 groups.

The agreement between calculated and observed data in West's paper would be considered excellent today, but it is even more striking when one considers that this work was published in 1930. Applying the usual 'reliability factor' R as a criterion of correctness of the structure:

$$R = \{\Sigma|F_o - F_c| \div \Sigma|F_o|\} \times 100\ ,$$

where the F_o are the observed and the F_c the calculated structure factors for the various reflecting planes, and the summations are over all planes concerned, the following values can be calculated from the data in West's paper:

$R = 8{\cdot}7$ for $(H0L)$ reflections;
$R = 6{\cdot}1$ for $(HK0)$ reflections.

These are excellent for a structure of this type.

(*B*) *The hydrogen positions*

Because of the low scattering power of hydrogen as compared with the other atoms in the structure, no actual evidence supporting the above location of the hydrogens appeared in West's Fourier analyses. It is now well known that Fourier difference syntheses (Cochran, 1951) can in some cases yield hydrogen positions. Normally the hydrogen contributions are so small that they are neglected in the calculation of structure factors. The observed structure factors contain the hydrogen contributions if the intensity data are accurate. If one subtracts the electron density distribution obtained by using the *calculated* structure factors as Fourier coefficients from that in which the *observed* values have been used, the hydrogen peaks should occur in the resulting difference map. Success with this method depends on factors such as the

* This choice by West is a 90° rotation about c from that listed in the *International Tables* for this space group. See *Internationale Tabellen zur Bestimmung von Kristallstrukturen*, (1944).

accuracy of the experimental observations and their reduction to structure factors, the densities of the other atoms in the structure, and the degree of refinement attained in positional and temperature-correction parameters. The difference method can itself be used to improve the last-mentioned parameters.

Upon calculation of the low values of R from West's data, the difference method was applied in an attempt to establish the hydrogen positions. Although the lower value of R was obtained for $(HK0)$ data, the heavy K and P peaks are superimposed in the projection on (001). Owing to this superposition, small errors in the P and K scattering curves could cause large ripples which 'wash out' the hydrogen peaks. The method was applied to $(H0L)$ data, since in the

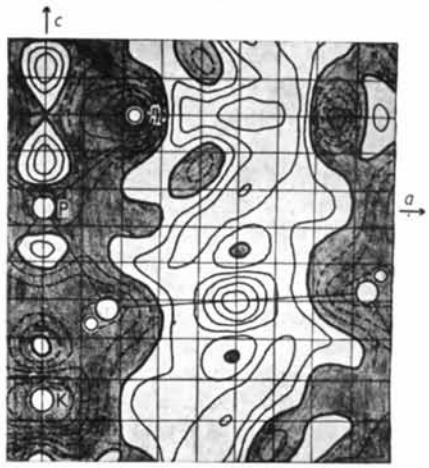

Fig. 2. (F_o-F_c) projection on (010) using West's data.

(010) projection the P and K peaks are separated by distances of $\frac{1}{4}c$.

A portion of the (F_o-F_c) projection of (010) is shown in Fig. 2. The shaded regions indicate negative and the unshaded regions positive values of the difference function. The P, K and O positions are shown as small unshaded circles. One notices a well-defined positive peak midway between two oxygens. This seems to check the selection of the 8-fold position given for hydrogen in Table 1, but offers no information on the parameter u. The behavior of the difference function in the neighborhood of the P, K and O positions shows that improvements could still be made. The negative peaks at these positions suggest that somewhat stronger temperature corrections, slightly anisotropic in the cases of P and K, would reduce the extraneous ripples and make the hydrogen peak more prominent. The hydrogen peak is extended in the direction of the bond.

It is possible that the method could be applied successfully to the (001) projection as well. Results obtained recently by neutron diffraction (R. Pepinsky & B. C. Frazer, unpublished) promise information far beyond the possibilities of the above procedure, however. The neutron study has demonstrated hydrogen peaks in a Fourier projection on (001), and suggests that the protons are disordered, with apparently two half-protons, on the average, in a double-minimum between the oxygen pair. This could account for the elongated electron cloud apparent in the difference of Fig. 2.

3. Preliminary considerations of the transition

(A) *The space groups*

Discussion of the tetragonal structure of KH_2PO_4 is usually in terms of the $I\bar{4}2d$ cell described in the preceding section. It is convenient to introduce the alternative $F\bar{4}d2$ representation of the tetragonal cell, in order to facilitate comparison with the Fdd symmetry below the Curie point. One obtains the $F\bar{4}d2$ cell from $I\bar{4}2d$ by choosing the base diagonals of the I cell as the a and b axes of the F cell and retaining the c axis. This doubles the volume of the cell and gives 8 KH_2PO_4 'molecules' per cell. The coordinates obtained by transforming those in Table 1 in this way are given in Table 2.

Table 2. *Coordinates in* $F\bar{4}d2$

$(0,0,0;\ \frac{1}{2},\frac{1}{2},0;\ \frac{1}{2},0,\frac{1}{2};\ 0,\frac{1}{2},\frac{1}{2})+$

8 P:	$0,0,0;\ \frac{1}{4},\frac{1}{4},\frac{3}{4}$.
8 K:	$0,0,\frac{1}{2};\ \frac{1}{4},\frac{1}{4},\frac{1}{4}$.
32 O:	$x,y,z;\ \frac{1}{4}-x,\frac{1}{4}+y,\frac{3}{4}+z;$
	$\bar{x},\bar{y},z;\ \frac{1}{4}+x,\frac{1}{4}-y,\frac{3}{4}+z;$
	$\bar{y},x,\bar{z};\ \frac{1}{4}+y,\frac{1}{4}+x,\frac{3}{4}-z$
	$y,\bar{x},\bar{z};\ \frac{1}{4}-y,\frac{1}{4}-x,\frac{3}{4}-z$
16 H:	$u,u-\frac{1}{4},\frac{1}{8};\ u+\frac{1}{4},\frac{1}{2}-u,\frac{1}{8};$
	$\frac{1}{2}-u,\frac{3}{4}-u,\frac{1}{8};\ \frac{1}{4}-u,u,\frac{1}{8}$.

The hydrogen-bonded system of PO_4 tetrahedra, as seen looking down the c axis in the $F\bar{4}d2$ cell, is shown in Fig. 3. The potassium positions are at a distance of $\frac{1}{2}c$ above and below the center of the tetrahedra. Thinking of the c axis as vertical, it is noticed that the hydrogen bonds always link an 'upper' oxygen of one PO_4 group to a 'lower' oxygen of a neighboring group.

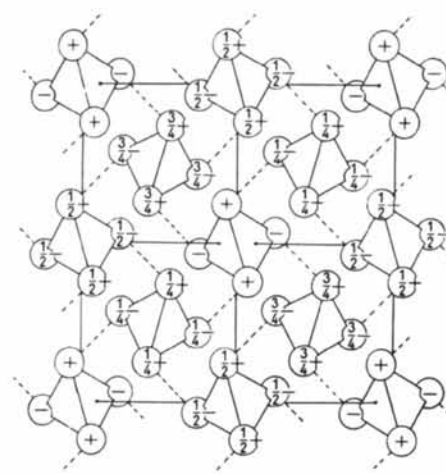

Fig. 3. The H_2PO_4 system in $F\bar{4}d2$.

The linkage is never 'upper' to 'upper' or 'lower' to 'lower'.

It is convenient here to review the basic feature of the Slater (1941) theory for the KH_2PO_4 transition. This theory assumes that both above and below the Curie point each PO_4 group has two closest H atoms, so that H_2PO_4 groups exist. Above the Curie point the two H's of an H_2PO_4 group are associated with any two of the four O's of a PO_4 tetrahedron (with the sole limitation that not more than one H will lie between two oxygens of neighboring PO_4 groups), so that the orientation of the H_2PO_4 groups is disordered. Below the Curie point ordering occurs, in such a way that ferroelectric domain hydrogens are associated more closely with only the 'upper' oxygens of all of the PO_4 groups, and in another domain only with the 'lower' oxygens. The H_2PO_4 dipoles, with their orientations parallel or anti-parallel to the c axis, are then presumed to account for the spontaneous polarization. An objection here is that the hydrogen bonds are nearly perpendicular to the direction of polarization, and could not of themselves account for charge displacement along the c axis. What is further required in Slater's model is that movement of the hydrogen causes some other ion or ions to be displaced in the c direction. The model is consistent with the *Fdd* symmetry found later by X-rays.

In a transition from the $F\bar{4}d2$ symmetry to that of *Fdd* the following changes occur:

(*a*) The equality of the a and b axes is no longer required.

(*b*) The $\bar{4}$ axes parallel to c become 2-fold axes.

(*c*) The 2-fold rotation and screw axes perpendicular to c are destroyed.

(*a*) permits a shear in the old $I\bar{4}2d$ cell. A shear of 27′ was measured by de Quervain (1944) and by Ubbelohde & Woodward (1947), and a value between 23′ and 30′ has been calculated by Yomosa & Nagamiya (1949). (*b*) and (*c*) permit the mechanism of the Slater model, and in addition permit other ionic displacements not there considered.

The atomic coordinates in *Fdd* are shown in Table 3. Both P and K become free in their z coordinate, but, as shown in Table 3, the P's have been chosen to define the lattice. The variable K parameter z_k is given as a displacement from the symmetry-fixed $F\bar{4}d2$ positions. The set of 32 equivalent oxygens in $F\bar{4}d2$ split into two non-equivalent 16-fold sets in *Fdd*. One of these consists of the 'upper' and the other the 'lower' oxygens. Hydrogens are then in 16-fold general positions.

Table 3. *Coordinates in Fdd*

	$(0,0,0;\ \frac{1}{2},\frac{1}{2},0;\ \frac{1}{2},0,\frac{1}{2};\ 0,\frac{1}{2},\frac{1}{2})+$
8 P:	$0,0,0;\ \frac{1}{4},\frac{1}{4},\frac{1}{4}$.
8 K:	$0,0,\frac{1}{2}+z_k;\ \frac{1}{4},\frac{1}{4},\frac{1}{4}+z_k$.
16 O:	$x_1,y_1,z_1;\ \frac{1}{4}+x_1,\frac{1}{4}-y_1,\frac{3}{4}+z_1;$
	$\bar{x}_1,\bar{y}_1,z_1;\ \frac{1}{4}-x_1,\frac{1}{4}+y_1,\frac{3}{4}+z_1;$
16 O:	$\bar{y}_2,x_2,\bar{z}_2;\ \frac{1}{4}+y_2,\frac{1}{4}+x_2,\frac{3}{4}-z_2;$
	$y_2,\bar{x}_2,\bar{z}_2;\ \frac{1}{4}-y_2,\frac{1}{4}-x_2,\frac{3}{4}-z_2$.
16 H:	$u,v,w;\ \frac{1}{4}-u,\frac{1}{4}+v,\frac{3}{4}+x;$
	$\bar{u},\bar{v},w;\ \frac{1}{4}+u,\frac{1}{4}-v,\frac{3}{4}+w$.

(*B*) *Structural nature of the problem*

The problem of gathering the necessary diffracted X-ray intensity data for solving the orthorhombic structure of KH_2PO_4 contains a complication which is not encountered in the usual crystal-structure determination. One is in effect simultaneously observing one half of the crystal in one position and the other half in a position rotated 90° about the c axis. This occurs because below the transition the crystal is not spontaneously polarized uniformly in one direction, but instead consists of many small domains which one may regard as being statistically polarized in directions parallel and anti-parallel to the c axis. A single reflection from what was an (HKL) plane in $F\bar{4}d2$ becomes simultaneously an (HKL) and a $(\bar{K}H\bar{L})$ reflection in *Fdd*. In general, these planes may differ both in interplanar spacing and in intensity of their diffraction maxima. If the difference in the interplanar spacing were large, and the two maxima could be resolved, there would be no problem. Resolution occurs only at relatively high angles, however, because the small shear of the old $I\bar{4}2d$ cell produces only a small difference in the orthorhombic a and b axes. It is fortunate that one important set of reflections exists for which the interplanar spacing and intensities of the pairs are equal. A difference does exist in the phase of the structure factors, but this is a computational, not an experimental, problem. The planes giving rise to this set of reflections are the (HHL) planes.

The set of (HHL) planes in *Fdd* and $F\bar{4}d2$ correspond to the complete set of $(0KL)$ planes in $I\bar{4}2d$. They are therefore the planes which would produce the zero layer line for an a-axis mounting in $I\bar{4}2d$, and if these observations were used in a Fourier synthesis one would obtain an electron-density projection on (100). As can be seen from Table 1 and Fig. 2, this single projection determines all three of the oxygen parameters. Moreover, a center of symmetry occurs in projection at $Y = 0$, $Z = \frac{1}{8}$, which simplifies the Fourier analysis. In $F\bar{4}d2$ and *Fdd* these data would yield a projection on (110), although the center of symmetry vanishes in the case of *Fdd*. The coordinates (r, s, t) measured on (110) could then be transformed so as to refer to the proper axis:

$$x = r+s;\ y = -r+s;\ z = t\,.$$

One difficulty does appear in the case of *Fdd*. The oxygen peaks necessary for determining s_1 and s_2 lie so close together that only an average of the two coordinates can be measured. It was possible to solve this s_1 and s_2 question in another manner.

If a sufficiently high field could be applied parallel to the c axis, it would be possible to align all of the domains in unidirectional polarization, and the (HKL) and $(\bar{K}H\bar{L})$ ambiguity could be removed. After some

experimental difficulties were surmounted, it was possible to mount a small crystal on its c axis for X-ray observation while a high field was maintained parallel to the c axis. This permitted the obtaining of distinct sets of x, y coordinates for the oxygens. Use of this technique with an $I\bar{4}2d$ a-axis mounting was not feasible, because of interference of the electrodes with the direct and diffracted X-ray beams.

The order of the experimental work differed from that described below. The ($HK0$) data were observed first, and the (HHL) data were obtained later by recording 126° K. $F\bar{4}d2$ and 116° K. Fdd reflections side by side on the same oscillation photographs, using a multi-layer-line screen with a movable camera. All observations were made with Zr-filtered Mo $K\alpha$ radiation. No corrections other than the Lorentz-polarization were made on the observed data, since both extinction and absorption were negligible. Temperature corrections were applied to the calculated structure factors. The Hartree atomic scattering curves tabulated in the *International Tables* (1944), with extension as given by Viervoll & Ögrim (1949), were used in all calculations.

4. The structure above the Curie point

(*A*) *Projection on* (110) *in* $F\bar{4}d2$

A crystal approximately $1{\cdot}0\times0{\cdot}2\times0{\cdot}25$ mm.^{3} in dimensions, with the long dimension parallel to the a axis, was mounted parallel to the rotation axis of the low-temperature goniometer. A complete set of oscillation photographs was taken, with observations above and below the transition temperature recorded on the same film for each oscillation range. A multi-layer-line shield was used in conjunction with a camera which could be moved parallel to the rotation axis. The exposures at the two temperatures, 116° K. and 126° K., were of equal length, and care was taken that the tube current remained constant. Several photographs at different exposure times were made for each of the 10° oscillation ranges. A 2° overlap insured the observation of all the reflections and permitted proper scaling of observations from different ranges. This procedure resulted in several measurements for every reflection.

Measurements of cell dimensions agreed to four figures with values calculated from thermal contraction data given by de Quervain (1944) and by Ubbelohde & Woodward (1947). These were later rechecked by differential comparison with room-temperature observations. The values found were:

	a (Å)	b (Å)	c (Å)
126° K. ($F\bar{4}d2$)	10·48	10·48	6·90
116° K. (Fdd)	10·53	10·44	6·90

By shifting the origin to the apparent center of symmetry at $Y=0$, $Z=\frac{1}{8}$, all of the phase angles for the (110) projection in $F\bar{4}2d$ were reduced to choices between 0 and 180°. It was assumed that the room-temperature parameters would not change by amounts sufficiently large to alter any of the signs except perhaps those of very weak reflections. The atomic scattering curves in these preliminary calculations were corrected for temperature by using an approximate temperature parameter determined from a few measurements by de Quervain (1944) and from the experimental scattering curves at room temperature determined by West.

A density projection was computed on X-RAC, (Pepinsky, 1947) assuming that the observed structure factors had the same signs as the corresponding calculated values. The new oxygen parameters obtained were then re-entered into the structure-factor calculations to check for changes in signs. Further positional refinements and the determination of more accurate temperature parameters were obtained from (F_o-F_c) syntheses, as discussed in the next section.

The final electron-density projection on (110) in $F\bar{4}d2$ is shown in Fig. 4, as photographed from X-RAC. The horizontal grid lines represent twentieths of the c axis, and the vertical lines are at fortieths of the $F\bar{4}d2$ base diagonal or twentieths of the a axis in $I\bar{4}2d$. The origin, at the apparent center of symmetry, is located near the center of Fig. 4(a). The heavy peaks on the central vertical coordinate line are superposed P and K maxima. The two nearest the center are the P peaks. The fairly high peaks on either side of the center of symmetry in the horizontal direction are superimposed oxygens from the two PO_4 groups. The horizontal distance of these peaks from the center of symmetry gives the s parameter in $F\bar{4}d2$. Finally, the small peaks are single oxygens, and their horizontal distances from the central vertical coordinate line measure the r parameter in $F\bar{4}d2$, while their vertical distances from the nearest phosphorus peaks measure the z parameter. Hydrogens connect the two superimposed oxygens by bonds nearly perpendicular to the plane of the figure, and connect by nearly horizontal bonds the single oxygen peaks near the center with those near the edge of the figure. Fig. 4(b) is an X-RAC enlargement of a portion of Fig. 4(a).

The final transformed oxygen coordinates obtained in the refinement described below were:

$$x = 0{\cdot}118,\ y = 0{\cdot}033,\ z = 0{\cdot}132\ .$$

A tabulation of the interatomic distances and discussion of the structure follows the analysis of the orthorhombic structure.

(*B*) *Refinement procedure*

It was clear in the beginning of the (F_o-F_c) syntheses that anisotropic temperature corrections would be necessary. This is evident, in fact, from the electron-density map itself. One can see distinct ellipticity in the peaks in Fig. 4. Ordinarily one corrects the atomic scattering power of an atom for

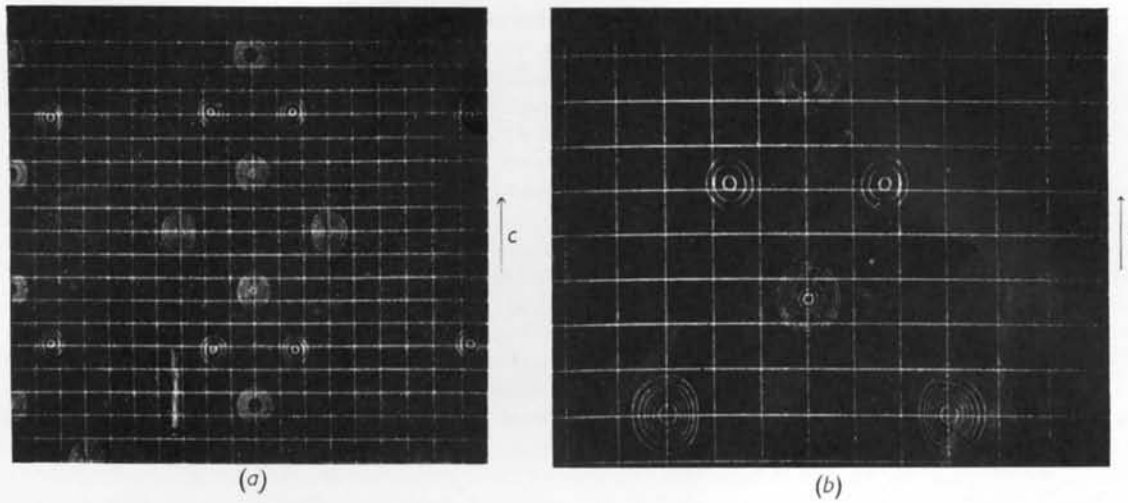

(a) (b)

Fig. 4. (a) Electron-density projection of KH_2PO_4 on (110) at 126° K. (b) Upper part of KH_2PO_4 asymmetric unit projected on (110) in *Fdd* at 126° K.

thermal agitation in a structure by determining a value of B in the equation

$$f_j = f_j^{(0)} \exp\left[-B_j s^2\right],$$

where j refers to the particular atom considered, s is the value of $\sin\theta/\lambda$ for the reciprocal-lattice point considered, and $f_j^{(0)}$ is the temperature-uncorrected scattering power of the atom for that value of s. The temperature correction parameter B_j is directly related to the actual thermal agitation by

$$B_j = 8\pi^2 \overline{U}_{jn}^2,$$

where U_{jn}^2 is the mean square displacement of the jth atom from its average position in a direction normal to the reflecting plane. Thus, while the magnitudes of the B's do not follow directly from the electron density map, the ellipticity of the peaks affords a means of determining fairly good ratios of the B's along the coordinate axes for any one atom. This ratio, which should be equal to the ratio of the squares of the major and minor axes, was found to be about 1·3 for all of the atoms. Actually the oxygen ellipses are not quite parallel to the axes, but were assumed to be so.

A certain amount of information was at hand for beginning the determination of the anisotropic B magnitudes. As mentioned earlier, an approximate value of B for all of the atoms was determined during the calculation of signs. This was about 0·5 Å^2. Furthermore, the ($00L$) and ($HH0$) reflections involve only the B's corresponding to the coordinate directions in Fig. 4(*a*), and these could be used not only to determine magnitudes but also to check the ratio derived from the peak ellipticities. In addition, use could be made of the three classes of structure factors:

(*a*) $\pm(P-K)\pm O$, H and L both odd;
(*b*) $\pm(P+K)\pm O$, H and L both even and $L=4n$;
(*c*) $\pm O$, H and L both even but $L\neq 4n$;

where the symbols, P, K and O represent the total contribution of the appropriate atoms. The final class permitted the atomic corrections for oxygen only. The approximate corrections for oxygen could then be used in (*a*) and (*b*), which taken together permitted separation of approximate P and K corrections. From these various sources, values were obtained for the B's as follows:

$B_{P,1} = 0{\cdot}36$ Å^{-2}	$B_{P,3} = 0{\cdot}47$ Å^{-2}
$B_{K,1} = 0{\cdot}30$	$B_{K,3} = 0{\cdot}40$
$B_{O,1} = 0{\cdot}45$	$B_{O,3} = 0{\cdot}55$

The first subscript refers to the kind of atom, and the second to whether B is to be used for ($HH0$) reflections (1) or to ($00L$) planes (3). The ratio of B's for any one atom does come out close to 1·3 Å^{-2}.

The B's for reflections from planes not perpendicular to the coordinate axes can conveniently be found by a simple geometrical construction. If $U_{P,1}$ and $U_{P,3}$ are the root-mean-square displacement components of a phosphorus atom along the coordinate directions parallel to the (110) plane of projection, then

$$B_{P,1} = 8\pi^2 U_{P,3}^2 \quad \text{and} \quad B_{P,3} = 8\pi^2 U_{P,1}^2 .$$

The U's define an ellipse in direct space. They also define an ellipse in reciprocal space, however, and this is much more conveniently used. Its semi-axes are proportional to $(B_{P,1})^{-\frac{1}{2}}$ and $(B_{P,3})^{-\frac{1}{2}}$. It is to be recalled that the reciprocal-lattice vector from the origin to a reciprocal-lattice point (corresponding to a plane of reflection) is perpendicular to that plane in direct space. Hence the value of U in the direction of the reciprocal-lattice vector is the value appropriate to the temperature parameter for the reflecting plane. Thus one can construct an ellipse in reciprocal space with semi-axes equal to $(B_{P,1})^{-\frac{1}{2}}$ and $(B_{P,3})^{-\frac{1}{2}}$ and obtain the proper $B_{P,HHL}$ from the radius vector

Table 4. *Structure factor comparison; (HHL) in* $F\bar{4}d2$

HHL	F_c	F_o	*HHL*	F_c	F_o	*HHL*	F_c	F_o
004	−14·0	−11·9	14,14,4	−13·3	−13·5	15,15,9	− 1·7	—
008	67·8	55·5	16,16,4	−24·6	−25·3	2,2,10	− 7·0	− 7·1
0,0,12	−11·3	−12·1	18,18,4	−17·6	−16·8	4,4,10	− 2·1	—
0,0,16	19·7	22·3	115	12·7	15·5	6,6,10	13·8	15·9
220	110·9	95·5	335	−14·9	−11·4	8,8,10	4·7	4·4
440	33·4	40·4	555	6·3	10·0	10,10,10	− 9·6	− 6·4
660	57·2	53·6	775	16·9	12·7	12,12,10	− 3·1	—
880	46·1	47·2	995	− 3·6	− 3·7	14,14,10	1·7	—
10,10,0	33·8	40·1	11,11,5	− 2·9	—	1,1,11	11·1	9·8
12,12,0	42·8	49·9	13,13,5	8·8	7·9	3,3,11	− 4·2	− 3·1
14,14,0	31·7	30·1	15,15,5	2·2	—	5,5,11	0·0	—
16,16,0	9·5	10·3	17,17,5	− 1·5	—	7,7,11	6·1	6·2
18,18,0	7·7	8·7	226	−13·6	−14·0	9,9,11	− 0·7	—
111	18·2	20·6	446	− 3·8	− 4·8	11,11,11	− 0·1	—
331	−48·4	−57·8	666	22·6	21·6	13,13,11	7·9	7·1
551	− 2·9	− 5·7	886	7·1	9·5	2,2,12	−23·2	−21·1
771	13·5	13·3	10,10,6	−13·9	−12·2	4,4,12	−31·1	−31·3
991	−11·0	− 8·8	12,12,6	− 4·5	− 3·4	6,6,12	−21·6	−25·1
11,11,1	− 9·0	− 9·4	14,14,6	2·4	—	8,8,12	−21·0	−15·9
13,13,1	4·5	5·1	16,16,6	− 1·2	—	10,10,12	−17·4	−14·8
15,15,1	− 3·4	—	117	9·8	9·3	12,12,12	− 7·6	− 5·5
17,17,1	− 6·9	− 9·7	337	−15·6	−12·3	1,1,13	3·0	5·6
222	−34·4	−39·2	557	− 5·8	− 2·2	3,3,13	− 2·7	—
442	− 7·4	− 9·3	777	3·8	5·7	5,5,13	5·7	8·6
662	34·9	37·4	997	− 8·1	− 8·1	7,7,13	9·4	11·5
882	9·7	11·3	11,11,7	− 0·9	—	9,9,13	− 1·0	—
10,10,2	−17·4	−18·1	13,13,7	5·1	4·5	11,11,13	− 2·6	—
12,12,2	− 5·5	− 6·5	15,15,7	− 2·8	− 2·7	13,13,13	2·8	2·9
14,14,2	2·9	—	17,17,7	− 6·7	− 7·4	2,2,14	− 3·9	—
16,16,2	− 1·4	—	228	44·5	42·6	4,4,14	− 1·2	—
113	33·3	31·5	448	24·8	22·1	6,6,14	8·0	10·2
333	−22·5	−27·2	668	33·2	30·3	8,8,14	2·7	—
553	1·5	2·9	888	28·7	27·9	10,10,14	− 5·6	− 7·5
773	15·0	13·9	10,10,8	22·0	20·2	1,1,15	− 2·2	—
993	− 4·3	− 3·5	12,12,8	28·6	30·3	3,3,15	− 6·0	− 5·8
11,11,3	− 0·6	—	14,14,8	22·0	26·8	5,5,15	− 4·4	—
13,13,3	11·7	12·0	16,16,8	6·0	5·2	7,7,15	− 0·6	—
15,15,3	1·8	—	119	− 0·7	− 4·7	9,9,15	− 3·3	—
17,17,3	− 3·4	− 3·6	339	−12·3	−11·5	2,2,16	12·0	14·0
224	−65·7	−70·2	559	0·6	—	4,4,16	7·6	7·9
444	−88·1	−86·5	779	7·1	7·3	6,6,16	11·6	10·2
664	−54·1	−53·5	999	− 7·2	−10·6	8,8,16	9·6	7·8
884	−44·4	−42·0	11,11,9	− 8·4	− 4·5	1,1,17	− 2·0	− 2·9
10,10,4	−38·4	−42·6	13,13,9	− 0·6	—	3,3,17	− 4·0	− 4·2
12,12,4	−15·9	−18·2						

$$\varrho = (B_{\mathrm{P},HHL})^{-\frac{1}{2}}$$

parallel to the reciprocal-lattice vector corresponding to (*HHL*).

The values of B given above for the various atoms were refined by several (F_o-F_c) syntheses (positional refinements were executed simultaneously). The final values were obtained by an application of the method of least squares. It was assumed for simplicity in this that the degree of anisotropy had been taken care of within the accuracy of the data, and thus that the final changes in the B's could be treated as small isotropic perturbations of the anisotropic B's already obtained. A brief description of the method follows.

One begins with the expression

$$F_o = (1+\Delta K)\sum_j f_j^{(0)} \exp\left[-(B_j+b_j)s^2\right] \cos\theta_j$$

or

$$F_o = (1+\Delta K)\sum_j f_j \exp\left[-b_j s^2\right] \cos\theta_j ,$$

where F_o is an observed structure factor approximately on an absolute scale; ΔK is the correction to absolute scale; f_j is the atomic scattering power of the jth atom for the proper value of s and with the approximate temperature correction parameter B_j; b_j is the isotropic correction for B_j; and $\cos\theta_j$ contains the positional effect of the jth atom on the total amplitude of the structure factor. By expanding the exponential and neglecting powers of b_j and products of b_j with ΔK, the equation can be rewritten:

$$F_o = \sum_j f_j \cos\theta_j + \Delta K \sum_j f_j \cos\theta_j - \sum_j f_j \cos\theta_j b_j s^2 .$$

But

$$F_c = \sum_j f_j \cos\theta_j = F_c^{(\mathrm{P})} + F_c^{(\mathrm{K})} + F_c^{(\mathrm{O})} ,$$

where F_c is the calculated structure factor corresponding to F_o, and $F_c^{(\mathrm{P})}$, $F_c^{(\mathrm{K})}$, and $F_c^{(\mathrm{O})}$ are the total contributions to F_c from the P, K and O atoms respectively.

One can then write

$$F_o - F_c = F_c \Delta K - s^2 F_c^{(P)} b_P - s^2 F_c^{(K)} b_K - s^2 F_c^{(O)} b_O \, .$$

There are as many such equations as there are structure factors. In an obvious way, one may form the four simultaneous equations for solution for the four unknowns ΔK, b_P, b_K and b_O:

$$\Sigma F_c(F_o - F_c) = \Sigma[F_c^2 \Delta K - s^2 F_c F_c^{(P)} b_P - s^2 F_c F_c^{(K)} b_K - s^2 F_c F_c^{(O)} b_O];$$

$$\Sigma s^2 F_c^{(P)}(F_o - F_c) = \Sigma[s^2 F_c^{(P)} F_c \Delta K - s^4 F_c^{(P)} b_P - s^4 F_c^{(P)} F_c^{(K)} b^K - s^4 F_c^{(P)} F_c^{(O)} b_O];$$

$$\Sigma s^2 F_c^{(K)}(F_o - F_c) = \Sigma[s^2 F_c^{(K)} F_c \Delta K - s^4 F_c^{(K)} F_c^{(P)} b_P - s^4 F_c^{(K)2} b_K - s^4 F_c^{(K)} F_c^{(O)} b_O];$$

$$\Sigma s^2 F_c^{(O)}(F_o - F_c) = \Sigma[s^2 F_c^{(O)} F_c \Delta K - s^4 F_c^{(O)} F_c^{(P)} b_P - s^4 F_c^{(O)} F_c^{(K)} b_K - s^4 F_c^{(O)2} b_O] \, .$$

The final values so obtained for the B's were

$$B_{P,1} = 0{\cdot}359 \text{ Å}^{-2} \quad B_{P,3} = 0{\cdot}485 \text{ Å}^{-2}$$
$$B_{K,1} = 0{\cdot}426 \quad B_{K,3} = 0{\cdot}552$$
$$B_{O,1} = 0{\cdot}439 \quad B_{O,3} = 0{\cdot}565$$

The F_c's were then recalculated with the appropriate values of the new B's, and the F_o's were rescaled by multiplying each of the old F_o's by $(1+\Delta K)^{-1}$. These quantities are compared in Table 4. A discussion of the correlation of the F's is given after the description of the structure below the Curie point.

5. The structure below the Curie point

(*A*) *Projection on* (001) *in Fdd*

The crystal used in gathering ($HK0$) data for an (001) projection of the orthorhombic structure was maintained in single-domain form during observation by application of an external electric field. This was accomplished by mounting a crystal of dimensions about $0{\cdot}2 \times 0{\cdot}2 \times 1{\cdot}0$ mm.^{3} in the manner shown in Fig. 5. A drop of conducting silver paint was used to stick the crystal to the copper goniometer head. After drying the paint thoroughly with a lamp, a simple jig with suitable centering and elevation adjustments was used to connect the fine high resistance wire lead to the lower end of the crystal. The bottom electrode was formed by closing a small loop at the end of the wire with silver paint. Just before the connection to the crystal was effected, another drop of paint was placed on the loop. After redrying, both connections were strengthened by coating the crystal and the electrodes with a thin quick-drying varnish.

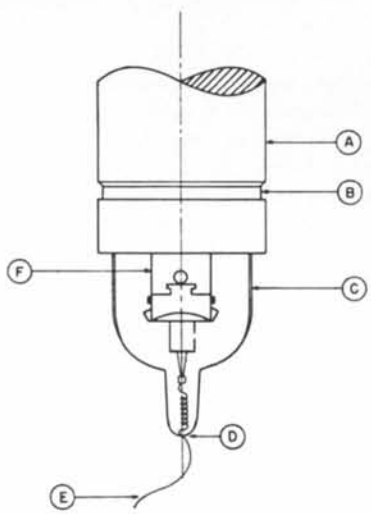

Fig. 5. Arrangement for applying electric field to crystal inside low-temperature Dewar vacuum. *A*: Goniometer dewar; *B*: Wood's-metal seal; *C*: glass bulb; *D*: picein seal; *E*: lead wire; *F*: copper goniometer head.

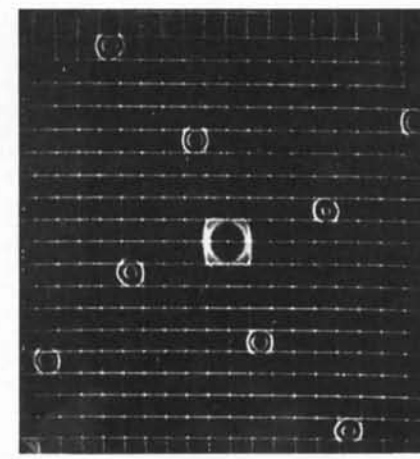

Fig. 6. KH_2PO_4 asymmetric unit projected on (001) at 116° K.

The crystal was oriented at room temperature with the vacuum-sealing bulb removed. The dewar was then sealed, and the possibility that the wire would introduce an excessive heat leak was checked by taking photographs at low temperature, without an applied field. The transition was still observed. A field of about 5000 V.cm.$^{-1}$ was maintained during subsequent oscillation photographs.

Signs were calculated for the observed structure factors on the assumption that the oxygen x and y parameters did not change in the transition. Trial projection on X-RAC and one more calculation were sufficient to fix all of the signs. The asymmetric unit from the final electron-density map is shown in Fig. 6. The heavy peaks are superimposed P and K peaks. The parameters for the two oxygens were

$$x_1 = 0{\cdot}114 \quad y_1 = 0{\cdot}034$$
$$x_2 = 0{\cdot}114 \quad y_2 = 0{\cdot}036$$

These sets were so nearly equal that it was assumed for the structure-factor comparison in Table 5 that

$$x_1 = x_2 = 0{\cdot}114, \quad \text{and} \quad y_1 = y_2 = 0{\cdot}035 \, .$$

The temperature corrections applied to the calculated structure factors in the table were the $B_{j,1}$ found for the (HHL) reflections discussed below.

Table 5. (*HK*0) *structure factor comparison* (*field applied*)

*HK*0	F_c	F_o	*HK*0	F_c	F_o	*HK*0	F_c	F_o
040	74·3	94·4	820	24·6	25·6	16,10,0	2·7	—
080	76·3	76·2	840	72·3	78·4	16,12,0	24·6	24·9
0,12,0	25·0	19·2	860	− 5·9	−11·1	16,14,0	1·6	—
0,16,0	28·8	26·2	880	42·9	45·3	16,16,0	13·0	18·8
0,20,0	20·4	16·9	8,10,0	14·1	15·7	16,18,0	− 4·9	—
0,24,0	19·0	17·9	8,12,0	31·5	28·7	16,20,0	13·9	10·1
0,28,0	16·0	10·2	8,14,0	− 5·1	—	16,22,0	− 3·6	—
400	74·5	96·9	8,16,0	20·4	22·5	16,24,0	11·1	7·3
800	76·8	83·2	8,18,0	− 0·9	—	18,2,0	34·2	33·0
12,0,0	24·9	20·7	8,20,0	19·1	16·9	18,4,0	− 4·1	—
16,0,0	29·3	26·8	8,22,0	− 3·2	—	18,6,0	29·0	26·2
20,0,0	20·6	16·0	8,24,0	16·6	12·9	18,8,0	0·9	—
24,0,0	19·2	15·8	8,26,0	− 1·8	—	18,10,0	14·9	10·4
28,0,0	16·3	11·1	8,28,0	12·3	7·0	18,12,0	− 4·8	—
220	113·2	138·2	10,2,0	60·8	62·5	18,14,0	14·8	11·2
240	−27·2	−25·0	10,4,0	− 5·8	—	18,16,0	4·9	—
260	63·8	65·2	10,6,0	52·6	49·0	18,18,0	8·0	10·5
280	−24·7	−26·3	10,8,0	−13·9	−15·0	18,20,0	− 2·1	—
2,10,0	60·5	56·2	10,10,0	30·3	29·0	18,22,0	13·4	7·3
2,12,0	− 1·2	—	10,12,0	2·3	—	20,2,0	−10·4	−16·3
2,14,0	29·4	25·8	10,14,0	28·6	33·8	20,4,0	22·9	17·0
2,16,0	0·6	—	10,16,0	− 2·7	—	20,6,0	− 0·6	—
2,18,0	34·0	33·2	10,18,0	14·8	19·2	20,8,0	19·2	17·8
2,20,0	10·4	15·0	10,20,0	9·6	—	20,10,0	− 9·6	—
2,22,0	13·3	11·1	10,22,0	19·9	12·4	20,12,0	18·6	20·6
2,24,0	1·8	—	10,24,0	− 0·9	—	20,14,0	3·2	—
2,26,0	17·5	13·9	10,26,0	10·6	7·6	20,16,0	13·9	13·8
2,28,0	1·5	—	12,2,0	1·2	—	20,18,0	2·1	—
420	27·2	26·8	12,4,0	49·4	45·2	20,20,0	10·7	10·1
440	38·8	34·9	12,6,0	−12·7	−14·4	22,2,0	13·4	10·8
460	−24·4	−24·1	12,8,0	31·5	27·1	22,4,0	− 1·4	—
480	72·1	76·7	12,10,0	− 2·3	—	22,6,0	15·8	16·6
4,10,0	5·8	—	12,12,0	41·4	42·8	22,8,0	3·2	—
4,12,0	49·1	43·1	12,14,0	− 1·8	—	22,10,0	20·0	17·6
4,14,0	− 4·3	—	12,16,0	24·6	27·2	22,12,0	− 3·6	—
4,16,0	41·7	40·7	12,18,0	4·7	—	22,14,0	16·6	13·3
4,18,0	4·0	—	12,20,0	18·5	15·8	22,16,0	3·6	—
4,20,0	22·7	20·4	12,22,0	3·5	—	22,18,0	13·5	7·7
4,22,0	1·4	—	12,24,0	10·2	10·5	24,2,0	− 1·8	—
4,24,0	11·4	16·6	14,2,0	29·6	28·0	24,4,0	11·6	12·9
4,26,0	− 0·3	—	14,4,0	4·4	—	24,6,0	9·1	—
4,28,0	7·2	6·7	14,6,0	37·4	34·6	24,8,0	16·8	9·8
620	63·9	72·8	14,8,0	5·1	—	24,10,0	0·9	—
640	24·3	25·3	14,10,0	28·8	27·8	24,12,0	10·3	8·7
660	57·3	63·0	14,12,0	1·9	—	24,14,0	1·7	—
680	5·9	11·2	14,14,0	36·1	31·5	24,16,0	11·2	6·8
6,10,0	52·6	49·6	14,16,0	− 1·7	—	26,2,0	17·7	11·7
6,12,0	12·7	11·0	14,18,0	14·8	16·9	26,4,0	0·3	—
6,14,0	37·2	36·8	14,20,0	− 3·2	—	26,6,0	11·4	8·0
6,16,0	−11·8	−10·5	14,22,0	16·5	11·8	26,8,0	1·8	—
6,18,0	28·8	28·0	14,24,0	− 1·6	—	26,10,0	10·6	—
6,20,0	0·6	—	16,2,0	− 0·6	—	28,2,0	− 1·5	—
6,22,0	15·6	15·4	16,4,0	42·0	42·6	28,4,0	7·5	6·7
6,24,0	− 8·9	—	16,6,0	11·8	10·4	28,6,0	− 3·9	—
6,26,0	11·3	7·7	16,8,0	20·5	19·0	28,8,0	12·5	6·5
6,28,0	3·8	—						

(*B*) *Projection on* (110) *in Fdd*

The center of symmetry at the coordinate origin in the (110) projection for $F\bar{4}d2$ is destroyed in the transition to *Fdd*. Making use of the results obtained from the preceding projection, and with certain crystal-chemical assumptions, it was possible to proceed rather directly with the analysis. All of the oxygen parameters except z_1 and z_2 had already been determined by the projection on (001). In addition, it was noticed that the greatest changes in observed intensities occurred for those reflections having both H and L odd. This was particularly useful in arriving at a trial structure for the first Fourier synthesis.

The structure factors for the (110) projection can be divided into the following classes:

(*a*) $\pm(P+K\exp[2\pi iLz_k])\pm(O_1\exp[2\pi iLz_1]+O_2\exp[-2\pi iLz_2])$ for H and L even but $L=4n$,

(*b*) $\pm(O_1\exp[2\pi iLz]+O_2\exp[-2\pi iLz_2])$ for H and L even and $L\neq 4n$,

(c) $\pm(P-K\exp[2\pi iLz_k])\pm(O_1\exp[2\pi iLz_1]+O_2\exp[-2\pi iLz_2])$ for H and L odd.

Since z_k is necessarily a small quantity, the P and K contributions are largely additive in (*a*), but subtractive in (*c*). Hence the changes in intensity due to z_k will evidently represent much higher percentages of the total intensity in (*c*) than in (*a*). With regard to (*b*): it is known from other structures involving PO_4 tetrahedra (modifications of P_2C_5, for example: de Decker & MacGillavry, 1941; de Decker, 1941) that considerable differences in the P, O bond character do not seriously alter the regularity of the O_4 tetrahedra. Hence one would expect z_1 and z_2 to differ by approximately equal but opposite amounts from the single parameter z in $F\bar{4}d2$. Since it had already been shown that the changes in the x and y parameters are quite small, the type (*b*) structure factors would be expected to differ in phase, but very little in magnitude, from those in $F\bar{4}d2$.

A structure was assumed, based on trial calculations involving only the odd reflections. This was used to calculate phases for the complete set of structure factors, and a projection was then made, using X-RAC. The pseudo-center at $Y = 0$, $Z = \frac{1}{8}$ was chosen as the projection origin. With the P's chosen to define the lattice, as in Table 3, the K's and O's were assumed to differ from their 126° K. positions, by a displacement of 0·04 Å in the c direction. The resulting density map gave the K peaks and the O_2 peaks in positions displaced further than assumed, and the O_1 peaks roughly in the assumed position.

Recognizing that a computed peak will lie between its assumed and its true position, new positions for K and O_2 were assigned. Several density maps were computed before the peaks settled in stable positions and the correctness ratio R stopped decreasing. At this point the (F_o-F_c) method was applied. Up to this time the temperature corrections determined above the Curie point had been used in the calculated structure factors. These gave fairly good agreement below the Curie point; but during the final (F_o-F_c) computations slightly different B's effected a further reduction in R. The values adopted were

$B_{P,1} = 0{\cdot}350$ Å^{-2}	$B_{P,3} = 0{\cdot}473$ Å^{-2}
$B_{K,1} = 0{\cdot}415$	$B_{K,3} = 0{\cdot}538$
$B_{O,1} = 0{\cdot}428$	$B_{O,3} = 0{\cdot}550$

The final electron-density map is shown in Fig. 7(*a*), and enlargements of the upper and lower portions are shown in Figs. 7(*b*) and 7(*c*) respectively. Comparing these with the 126° K. projection in Figs. 4(*a*) and 4(*b*), it is seen that the P peaks remain half-way between grid lines on the c axis (as they should, since these atoms were chosen to define the lattice), but shifts in the c direction are clearly seen for the K and O peaks.

It is to be recalled that the superposition of two

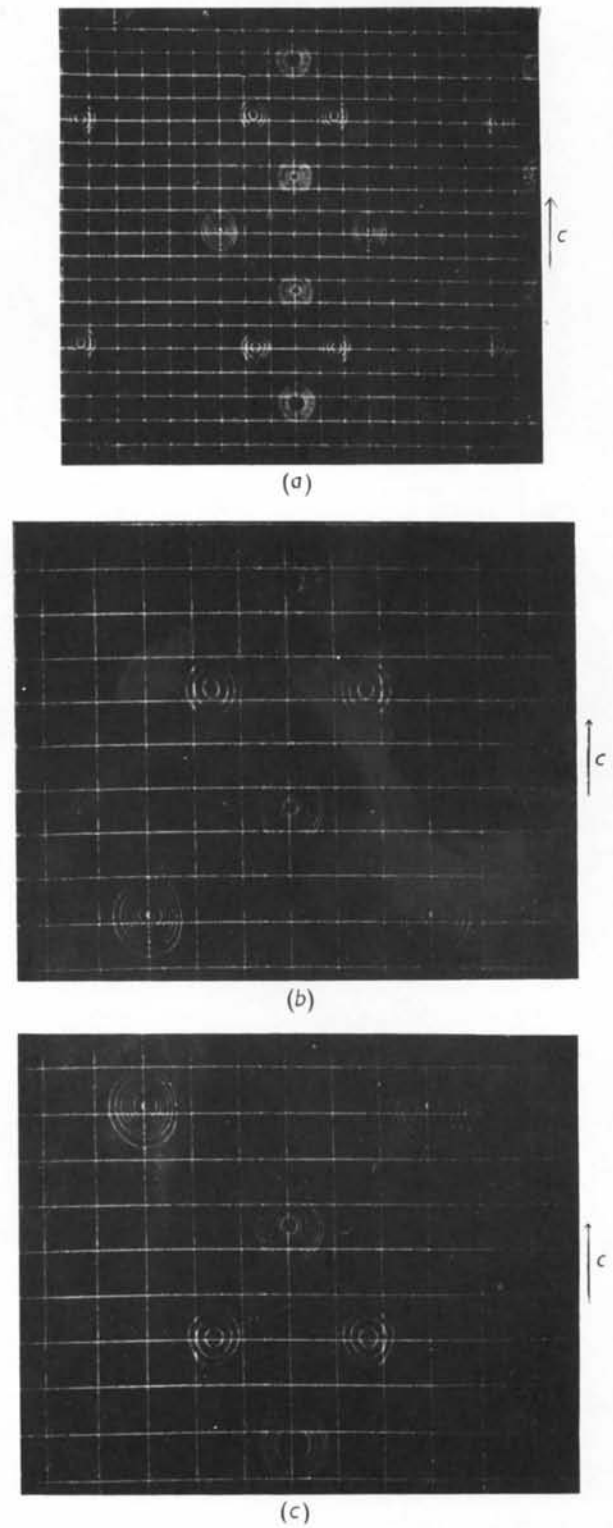

Fig. 7. (*a*) Electron-density projection of KH_2PO_4 on (110) at 116° K. (*b*) Upper portion of KH_2PO_4 asymmetric unit projected on (110) in $F\bar{4}d2$ at 116° K. (*c*) Lower portion of KH_2PO_4 asymmetric unit projected on (110) in *Fdd* at 116° K.

Table 6. *Structure factor comparison*; (*HHL*) *in Fdd*

HHL	Cos	Sin	$\|F_c\|$	$\|F_o\|$	*HHL*	Cos	Sin	$\|F_c\|$	$\|F_o\|$
004	−0·96	−0·25	12·9	12·0	557	−0·25	−0·98	8·7	8·8
008	0·95	0·31	67·2	56·0	777	0·74	−0·68	8·0	10·5
0,0,12	−0·78	−0·62	8·3	12·2	997	−0·67	−0·74	10·7	9·4
0,0,16	0·79	0·62	18·9	22·5	11,11,7	−0·58	−0·82	7·2	2·8
220	1·00	0·00	112·1	96·3	13,13,7	0·94	−0·36	6·1	7·0
440	1·00	0·00	36·5	40·7	15,15,7	−0·56	−0·84	4·3	3·7
660	1·00	0·00	58·1	54·1	17,17,7	−0·83	−0·57	6·9	8·7
880	1·00	0·00	45·0	47·6	223	0·95	0·32	43·4	43·1
10,10,0	1·00	0·00	32·6	40·5	448	0·94	0·34	24·1	21·8
12,12,0	1·00	0·00	44·4	50·4	668	0·95	0·33	32·4	30·6
14,14,0	1·00	0·00	34·0	32·0	888	0·94	0·34	26·4	28·3
16,16,0	1·00	0·00	11·5	11·6	10,10,8	0·94	0·35	20·3	19·0
18,18,0	1·00	0·00	8·8	8·4	12,12,8	0·95	0·33	29·3	30·6
111	1·00	−0·08	18·7	20·8	14,14,8	0·95	0·33	23·1	29·7
331	1·00	−0·08	50·6	56·5	16,16,8	0·93	0·39	6·7	7·7
551	−0·70	−0·75	3·6	5·8	119	0·39	−0·92	8·9	11·3
771	1·00	−0·07	12·4	13·4	339	−0·60	−0·80	15·6	12·2
991	−0·99	−0·14	11·6	9·9	559	0·31	−0·95	7·7	9·0
11,11,1	−0·99	−0·14	8·7	9·5	779	0·90	−0·44	9·5	10·4
13,13,1	0·96	−0·26	4·6	5·5	999	−0·58	−0·82	9·2	10·7
15,15,1	−0·99	−0·15	4·1	—	11,11,9	−0·62	−0·79	8·9	6·5
17,17,1	−1·00	−0·09	6·8	9·8	13,13,9	0·65	−0·78	4·0	—
222	−1·00	−0·07	36·4	40·4	15,15,9	−0·44	−0·95	3·9	—
442	−1·00	0·08	8·9	9·4	2,2,10	−0·93	−0·37	7·9	7·2
662	1·00	0·08	35·2	37·8	4,4,10	−0·93	−0·37	2·7	—
882	1·00	0·08	10·7	11·4	6,6,10	0·93	0·37	15·0	14·8
10,10,2	−1·00	−0·08	15·7	18·0	8,8,10	0·93	0·36	5·6	4·9
12,12,2	−1·00	−0·08	4·9	6·6	10,10,10	−0·93	−0·37	9·1	6·5
14,14,2	0·99	0·14	0·7	—	12,12,10	−0·94	−0·37	3·0	—
16,16,2	−1·00	−0·06	3·3	—	14,14,10	0·89	0·45	0·4	—
113	0·96	0·30	34·9	31·9	1,1,11	0·49	0·88	12·8	12·6
333	−0·99	0·14	23·3	27·4	3,3,11	0·82	0·58	9·3	10·2
553	0·46	0·90	5·7	5·9	5,5,11	−0·29	0·97	6·3	8·5
773	0·94	0·35	15·9	14·0	7,7,11	0·40	0·93	9·2	12·6
993	0·90	0·46	5·7	5·0	9,9,11	−0·64	−0·78	5·5	—
11,11,3	−0·20	0·99	2·5	—	11,11,11	−0·13	1·00	4·7	—
13,13,3	0·96	0·25	12·4	13·2	13,13,11	0·66	0·75	9·0	9·0
15,15,3	0·70	0·74	2·3	—	2,2,12	0·89	−0·53	20·4	20·2
17,17,3	−0·97	0·28	2·9	3·6	4,4,12	−0·88	−0·49	29·4	32·7
224	−0·99	−0·17	64·6	70·9	6,6,12	0·83	−0·51	20·1	25·3
444	−0·99	−0·16	86·3	87·3	8,8,12	−0·89	−0·50	20·8	16·1
664	−0·99	−0·16	53·7	54·0	10,10,12	−0·87	−0·50	17·4	14·9
884	−0·99	−0·16	46·8	42·4	12,12,12	−0·82	−0·58	5·9	5·6
10,10,4	−0·99	−0·17	40·2	42·7	1,1,13	0·08	1·00	8·0	8·8
12,12,4	−0·98	−0·19	15·6	19·6	3,3,13	−0·83	0·56	7·5	7·9
14,14,4	−0·98	−0·19	12·5	12·2	5,5,13	0·13	1·00	7·9	9·4
16,16,4	−0·99	−0·17	24·3	26·8	7,7,13	0·51	0·85	10·9	12·9
18,18,4	−0·98	−0·17	18·1	17·1	9,9,13	−0·63	0·78	4·9	—
115	0·75	0·66	16·5	15·7	11,11,13	−0·81	0·60	4·7	—
335	−0·97	0·27	17·3	12·8	13,13,13	0·29	0·96	4·9	5·9
555	0·50	0·87	9·0	10·1	2,2,14	−0·87	−0·50	4·6	—
775	0·84	0·55	15·3	12·7	4,4,14	−0·88	−0·50	1·6	—
995	−0·76	0·66	5·9	6·6	6,6,14	0·87	0·51	9·1	11·2
11,11,5	−0·63	0·79	4·3	—	8,8,14	0·88	0·52	3·3	—
13,13,5	0·88	0·47	10·1	9·3	10,10,14	−0·86	−0·51	5·7	7·6
15,15,5	0·30	0·99	2·7	—	1,1,15	0·83	−0·49	6·6	4·7
17,17,5	−0·83	0·61	2·3	—	3,3,15	−0·28	−0·97	8·3	11·3
226	−0·98	−0·23	16·7	14·1	5,5,15	−0·02	−0·99	6·3	3·0
446	−0·98	−0·22	4·6	4·8	7,7,15	0·60	−0·83	4·7	—
666	0·98	0·23	23·3	21·9	9,9,15	−0·31	−0·96	5·5	7·2
886	0·98	0·22	8·2	9·6	2,2,16	0·76	0·66	11·4	14·1
10,10,6	−0·98	−0·23	12·5	11·5	4,4,16	0·69	0·73	5·5	8·0
12,12,6	−0·98	−0·23	4·8	2·8	6,6,16	0·76	0·67	9·0	10·3
14,14,6	0·86	0·14	0·7	—	8,8,16	0·75	0·67	7·5	7·9
16,16,6	−0·96	−0·21	2·8	—	1,1,17	0·47	−0·88	4·3	5·5
117	0·86	−0·51	12·5	11·2	3,3,17	−0·20	−0·98	4·9	5·8
337	−0·73	−0·69	18·1	13·1					

oxygens in the two peaks near the central horizontal grid line precludes separate measurement of s_1 and s_2. It was assumed that $s_1 = s_2$, and this was supported by the (*HK*0) results obtained earlier. r_1 and r_2, which can be measured separately from the single oxygen peaks, were found to be equal.

The complete set of parameters obtained was

O_1: $x_1 = 0{\cdot}117$, $y_1 = 0{\cdot}035$, $z_1 = 0{\cdot}136$;
O_2: $x_1 = 0{\cdot}117$, $y_1 = 0{\cdot}035$, $z_2 = 0{\cdot}124$;
K: $z_k = 0{\cdot}012$.

The structure factors are compared in Table 6.

6. Discussion of results

The correctness ratios calculated from Tables 4–6 are

$R = 12{\cdot}1$ for (*HHL*) in $F\bar{4}d2$;
$R = 13{\cdot}5$ for (*HK*0) in *Fdd*;
$R = 11{\cdot}8$ for (*HHL*) in *Fdd*.

In obtaining these values the zero observations were not considered. When the zero observations were included, by arbitrarily assuming that their structure factors had a value equal to half of the lowest actually observed structure factor, the *R*'s increased to the values

$R = 13{\cdot}9$ for (*HHL*) in $F\bar{4}d2$;
$R = 16{\cdot}3$ for (*HK*0) in *Fdd*;
$R = 13{\cdot}8$ for (*HHL*) in *Fdd*.

The two structure determinations and the room-temperature structure are compared in Table 7. The interatomic distances for the latter were calculated on the basis of the West oxygen parameters and Ubbelohde & Woodward's cell dimensions. In tabulating the *x* parameter for oxygen in *Fdd*, somewhat more weight was attached to the (*HHL*) results because of the lower value of *R*. In the tabulation of interatomic distances, P, O refers to the bond lengths in the PO_4 groups; O, O is the distance between oxygens having the same *c* elevation in a PO_4 group; O, O′ is the distance between those of opposite elevation relative to the central P atom; O–H · · · O symbolizes the hydrogen bond lengths; K, O is the distance from a potassium to the oxygen neighbors which belong to phosphorous atoms having the same (*X*, *Y*) coordinates; and K, O′ refers to those belonging to P's displaced from K by $(\pm\frac{1}{4}, \pm\frac{1}{4})$ in the *X* and *Y* directions. The double values occurring in some cases in the 116° K. structure have been arranged so that the upper value involves the O_1 oxygens and the lower value the O_2 oxygens.

Table 7. *Comparison of structures*

		Room temp.	126° K.	116° K.
O:	*x*	0·112	0·118	0·116 0·116
	y	0·032	0·033	0·035 0·035
	z	0·139	0·132	0·136 0·124
K:	z_k	0	0	0·012
	P, O	1·56 Å	1·57 Å	1·58 Å 1·53
	O, O	2·45	2·57	2·55 2·53
	O, O′	2·59	2·57	2·54
O–H · · ·	O	2·53	2·44	2·51
	K, O	2·79	2·85	2·89 2·81
	K, O′	2·82	2·79	2·79 2·78
	a	10·512 Å	10·48 Å	10·53 Å
	b	10·512	10·48	10·44
	c	6·945	6·90	6·90

On cooling from room temperature to 126° K. it is noticed that the somewhat elongated PO_4 tetrahedra assume a regular shape. In addition, two particularly interesting changes occur in other distances. One of these is a marked contraction of the hydrogen bonds. The other is observed in the distinct difference between K, O and K, O′. The elongated K, O distance has its principal component parallel to the *c* axis. It is just along this direction that preferential vibration was found earlier, and it is also the direction of spontaneous polarization.

Below the transition temperature the O's form a practically regular tetrahedron, but the P has 'sagged' from its central position. The displacement of P is about 0·03 Å. An interesting expansion of the hydrogen bond is observed in the transition. This and the K displacement appear to be most significant results of the study. The latter is 0·08 Å relative to the nearest P's and 0·05 Å relative to the corresponding O_4 tetrahedra.

It is clear that the theoretical aspects of ferroelectricity for the KH_2PO_4-type crystals must be re-

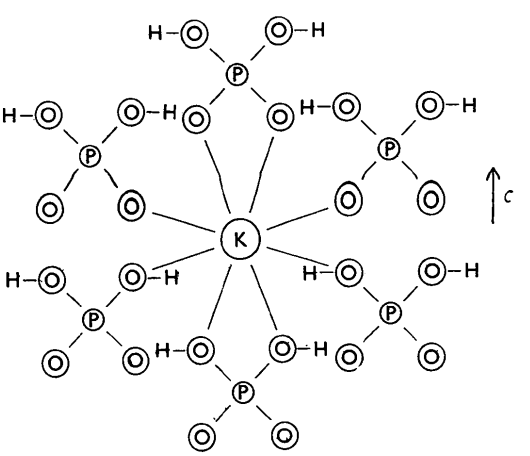

Fig. 8. Neighborhood of potassium atoms.

vised; however, Slater's assumption regarding the ordering of the hydrogens appears to be reasonable. In the first place, the expansion of the hydrogen bond in the transition supports such a view. In addition, if one assumes that the hydrogens 'belong' to the O_1 set of oxygens, and have been 'lost' by the O_2 set, then the observed lengthening of P, O_1 and contraction of P, O_2 could be a reasonable consequence. Furthermore, the change in the ionic environment of the K's would act so as to displace them in the proper direction. This is evident from Fig. 8, in which the neighborhood of the K's is shown schematically.

The question remains as to how these changes could be 'triggered' in the transition. The hydrogen role has been emphasized heretofore, but a more complete answer might be the following. As the crystal is cooled, the hydrogen bonds begin to contract in the X, Y plane. The effect of this is to destroy the equidistance of the KO_8 arrangement. This causes the K to build up a preferred vibration parallel to c, which in turn induces a similar preferred vibration in the PO_4 groups. Finally a critical temperature is reached, the Curie point, at which the K's 'lock in' to a position displaced from their previous centers of oscillation. The displaced K's then exert a polarizing influence on the PO_4 groups and an electrostatic influence on the hydrogens. In this way the P's become displaced within their O_4 tetrahedra and the hydrogens become more ordered.

The tentative model just described, or other such models that seem to fit the structural results reported here, will depend on future verification of the structural role of the hydrogens in the transition. The best approach to this seems to be through neutron diffraction. The results of the present investigation will greatly simplify such work, and should facilitate more extensive theoretical treatment of the general problem of the KH_2PO_4-type ferroelectrics as well.

References

Busch, G. & Scherrer, P. (1935). *Naturwissenschaften*, **23**, 737.

Cochran, W. (1951). *Acta Cryst.* **4**, 81.

Decker, H. C. J. de (1941). *Rev. Trav. chim. Pays-Bas*, **60**, 414.

Decker, H. C. J. de & MacGillavry, C. H. (1941). *Rec. Trav. chim. Pays-Bas*, **60**, 153.

Frazer, B. C. & Pepinsky, R. (1950). *Phys. Rev.* **80**, 124.

Internationale Tabellen zur Bestimmung von Kristallstrukturen (1944), revised ed. Ann Arbor: Edwards.

Pepinsky, R. (1947). *J. Appl. Phys.* **18**, 601.

Quervain, M. de (1944). *Helv. phys. Acta*, **17**, 509.

Slater, J. C. (1941). *J. Chem. Phys.* **9**, 16.

Ubbelohde, A. R. & Woodward, I. (1947). *Proc. Roy. Soc.* A, **188**, 358.

Viervoll, H. & Ögrim, O. (1949). *Acta Cryst.* **2**, 277.

West, J. (1930). *Z. Krystallogr.* **74**, 306.

Yomosa, S. & Nagamiya, T. (1949). *Prog. Theor. Phys.* **4**, 263.

Acta Cryst. (1953). **6**, 285

The Structure of $MnAl_6$

By A. D. I. Nicol

Crystallographic Laboratory, Cavendish Laboratory, Cambridge, England and B.S.A. Group Research Centre, Sheffield, England

(*Received* 21 *October* 1952)

The structure of the compound $MnAl_6$ has been determined. A brief description is given of the experimental methods used, together with an estimate of the accuracy obtained in the structure analysis. Electron counts and Brillouin zone measurements provide qualitative evidence in support of Raynor's theory that in electron-rich phases the transitional metal atoms absorb electrons. Some interesting Mn–Al and Al–Al interatomic distances are discussed in detail and it is suggested that they, too, provide indirect evidence of the importance of electronic factors in the formation of this structure.

1. Introduction

The determination of the structure of $MnAl_6$ forms part of a programme of structural work on the aluminium-rich phases occurring in binary and ternary alloys of aluminium with the transitional metals of the first long period. The work of Raynor and his collaborators in Birmingham (see, for example, Raynor & Wakeman, 1947; Raynor & Waldron, 1948; Pratt & Raynor, 1951) has indicated that the investigation of these alloys is likely to be important for the further theoretical study of alloy formation. The present research was undertaken with the intention of helping to establish some of the factors which govern the formation of these stable intermetallic compounds.

Assuming that these phases may be regarded as